RSC Advances

ROYAL SOCIETY OF CHEMISTRY

www.rsc.org/advances

Synthesis and Characterization of Polyfluorene-based Photoelectric Materials: the Effect of Coil Segment on the Spectral Stability

Jin-Jin Li[1], Jian-Jian Wang[2], Yin-Ning Zhou[1], Zheng-Hong Luo[1, 2*]

[1]*Department of Chemical Engineering, School of Chemistry and Chemical Engineering, Shanghai Jiao Tong University, Shanghai 200240, P. R. China*

[2]*Department of Chemical and Biochemical Engineering, College of Chemistry and Chemical Engineering, Xiamen University, Xiamen 361005, P. R. China*

* Correspondence to: Prof. Z.H. Luo; e-mail: luozh@sjtu.edu.cn

Tel.: +86-21-54745602

Fax: +86-21-54745602

Abstract:

The origin of the low-energy emission of fluorene-based rod-coil block copolymers still remains controversial. In this work, a series of polyfluorene-based rod-coil block copolymers having different coil segments, *i.e.*, poly[2,7-(9,9-dihexylfluorene)]-*block*-poly(2,2,3,3,4,4,4-heptafluorobutyl methacrylate, (PF-*b*-PHFBMA), PF-*b*-poly(butyl methacrylate) (PF-*b*-PBMA), PF-*b*-poly(2-hydroxyethyl methacrylate) (PF-*b*-PHEMA) and PF-*b*-poly(acrylic acid) (PF-*b*-PAA), were well synthesized using ATRP technique. The optical, surface properties and thermal behaviors of these copolymers were systematically investigated. Especially, different thermal treatment conditions, including annealing temperature, annealing time and annealing atmosphere were introduced to study the effect of coil segment on the copolymer spectral stability. The incorporation of PBMA, PHEMA and PAA segments to PF could indeed improve the copolymer spectral stability, while PHFBMA block brought the undesirable low-energy emission. In addition, water contact angle (WCA) measurement of the copolymer films before and after annealing further demonstrated that the low-energy emission of PF-based rod-coil block copolymers was attributed to the molecular aggregation rather than the formation of fluorenone defects.

Keywords:

Polyfluorene-based rod-coil block copolymers; molecular aggregation; low-energy emission; spectral stability

Introduction

Fluorene-based polymers (PFs) have been intensively studied as blue-light-emitting materials in polymer light-emitting diodes (PLEDs) due to high photoluminescence efficiency, good photostability and the emission of polarized blue light.[1-5] The poor spectral stability under thermal treatment or passage of current caused to the appearance of a low-energy emission band at 520-530 nm significantly limited their application in blue PLEDs.[4, 5] Three models, *i.e.*, the creation of keto defects in the backbone of PFs,[6-8] the formation of aggregates or intermolecular excimer emission[9-11] as well as the combination of the two mechanisms,[12,13] have been suggested to clarify this phenomenon. The exact origin of this low-energy emission band remains unclear.[14] Nevertheless various efforts have been made to address this disadvantage, including using either dendrimers or bulky substituents in the 9-position of the fluorine moiety,[15,16] copolymerization techniques,[17,18] purification of the fluorine monomers before polymerization,[19] or blends of PFs with some nonconjugated polymers such as polystyrene (PS) or poly(vinyldiphenylquinoline),[20] while the undesirable emission band was not eliminated.[21]

In recent studies, coil-like blocks nonconjugated and hole/electron transporting molecules were incorporated into polyfluorene backbones to suppress the aforementioned low-energy emission.[21-24] So far, many coil segments have been used to form PF-based rod-coil block copolymers, such as poly (methyl methacrylate) (PMMA), polystyrene (PS), poly(2-hydroxyethyl methacrylate) (PHEMA),

poly(2-(dimethylamino)ethyl methacrylate) (PDMAEMA) and poly(ethylene oxide) (PEO).[25-30] The aggregation and microphase separation behavior of these block copolymers caused to the incompatibility of rod and coil segments can lead to the formation of unusual nanoscale morphologies and photophysical properties in both solution and solid state.[14,31] These functions, which can be adjusted flexibly through introducing different coil segments, have attracted great attention for optoelectronic or sensory applications.[32,33] However, the influence of coil segments related to the microphase separation behavior on the photophysical properties of PF-based rod-coil block copolymers has not been fully explored.

Recently, we have synthesized a series of PF-based rod-coil block copolymers with PHFBMA as the coil segment by ATRP and reported that the micelle structure formed by different selective solvents has a dramatic influence on their optical properties.[34] The previous study was achieved in solution, however the influence of separation behavior on the optical properties of these block copolymers in solid state has not ever been studied. Based on this idea, four coil segments having different polarity and solubility are selected to form PF-based rod-coil block copolymers PF-*b*-PHFBMA, PF-*b*-PBMA, PF-*b*-PHEMA and PF-*b*-PAA in this study. These copolymers with a similar polymerization degree are well synthesized through ATRP technique. **Scheme 1** shows the synthetic routes and corresponding synthetic conditions. Particular attention is focused on the effect of coil segment on the copolymer spectral stability under different thermal treatment conditions. In addition, water contact angle (WCA) measurements about the surface properties and thermal

stability of resulting polymers were also carried out.

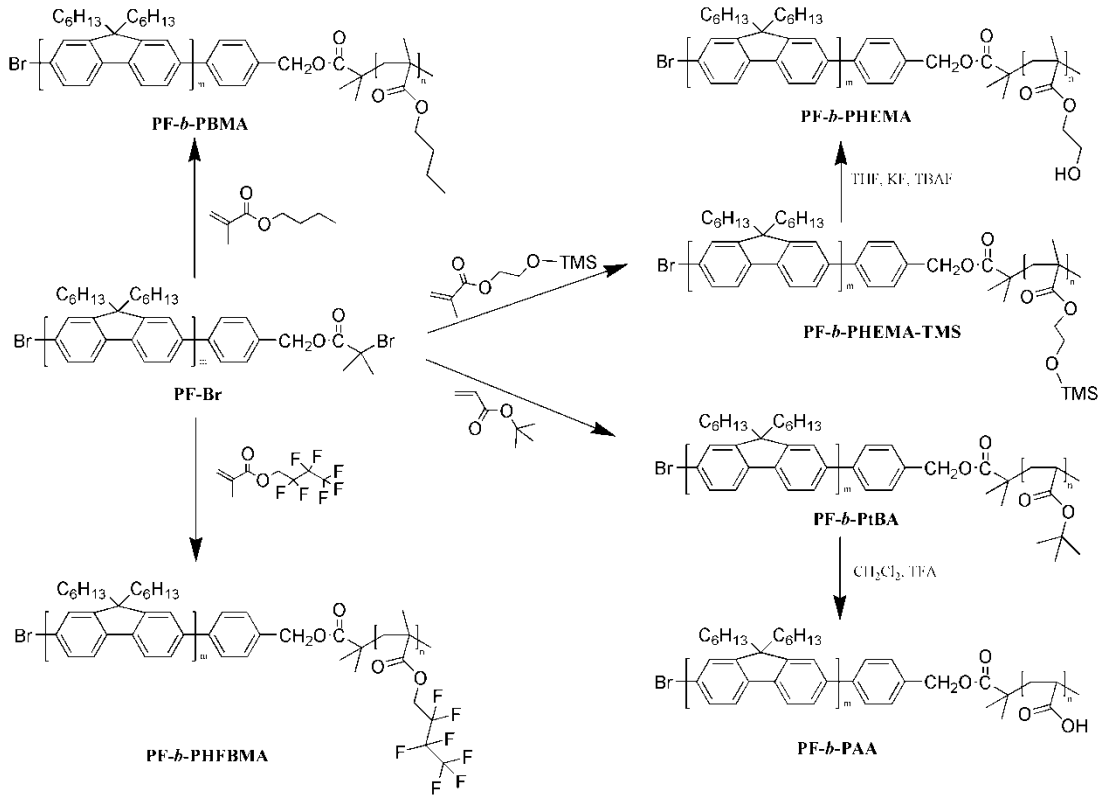

Scheme 1. Synthesis Route of polyfluorene-based rod-coil block copolymers PF-*b*-PHFBMA, PF-*b*-PBMA, PF-*b*-PHEMA, PF-*b*-PAA.

Experimental Section

Materials

α-{4-[2-(2-bromo-2-methylpropoyloxy)methyl]phenyl}-ω-bromo-poly[2,7-(9,9-dihexyl-fluorene)] (PF-Br) was synthesized using a similar procedure, which has been reported by Chen et al.[29] and us[34]. 1,1,4,7,7-Pentamethyldiethylenetriamine (PMDETA, 98%) was purchased from Aldrich. 2-Hydroxyethyl methacrylate (HEMA, 95%) and tetrabutylammonium fluoride (TBAF, 1M in tetrahydrofuran) were obtained from TCI (Shanghai) Development. HEMA was purified by washing an aqueous solution of monomer with hexane to remove ethylene glycol dimethacrylate, salting the monomer out of the aqueous phase by addition of NaCl, drying over $MgSO_4$, and distilling under

reduced pressure. Potassium fluoride (KF, 99%), trifluoroacetic acid (TFA, 99%), copper(I) chlorine (CuCl, 98%), butyl methacrylate (BMA, AR) were obtained from Sinopharm Chemical Reagent (SCRC). 2,2,3,3,4,4,4-Heptafluorobutyl methacrylate (HFBMA, 98%) was obtained from A Better Choice for Research Chemicals GmbH & Co. KG. (ABCR). Tert-butyl acrylate (*t*BA, 99%) was purchased from Aladdin. BMA, HFBMA and *t*BA were washed with 5wt% aqueous NaOH solution to remove inhibitor before polymerization. All other reagents and solvents were obtained from SCRC and used without further purification.

Synthesis of PF-*b*-PHFBMA

100 mg (0.017 mmol) PF-Br first dissolved in 2.5 mL of cyclohexanone, 14.2 μL PMDETA and 3.4 mg CuCl were added to the solution. The mixture was degassed and then filled with nitrogen three times at 0 °C, followed by addition of 339μL (1.7 mmol) HFBMA. Finally, the flask was immersed into an oil bath preheated at 80 °C for 24h. The polymerization was terminated by opening the flask and exposing the mixture to air. After cooling to room temperature, the copolymer solution was diluted with THF and passed through an alumina column to remove the catalyst. Finally, the resulting solution was concentrated and poured into methanol to precipitate the product. The product was further purified twice by redissolving/reprecipitating with THF/ methanol and dried in vacuum for 24 h to obtain PF-*b*-PHFBMA.

Synthesis of PF-*b*-PBMA

The synthesis process was the same as the synthesis process of PF-*b*-PHFBMA except replacing HFBMA by BMA (270 μL, 1.7 mmol).

Synthesis of PF-*b*-PAA

PF-*b*-P*t*BA was first prepared using PF-Br as macroinitiator and *t*BA as monomer. The synthesis process was the same as the synthesis process of PF-*b*-PHFBMA except replacing HFBMA by *t*BA (370 μL, 1.7 mmol). Then the obtained copolymer PF-*b*-P*t*BA (60 mg) was dissolved in 15 mL dry dichloromethane. 6.5 μL TFA was added and the solution was stirred at room temperature for 24 h. A precipitate was obtained after pouring the concentrated solution into n-hexane. The result copolymer PF-*b*-PAA was dried under vacuum for 24 h.

Synthesis of PF-*b*-PHEMA

2-(trimethylsilyl)ethyl methacrylate (HEMA–TMS) instead of HEMA is usually used to synthesize block copolymers due to its high solubility in organic media.[35] PF-*b*-P(HEMA-TMS) was first prepared using PF-Br as macroinitiator and HEMA-TMS as monomer. The synthesis process was the same as the synthesis process of PF-*b*-PHFBMA except replacing HFBMA by HEMA-TMS (354 μL, 1.7 mmol). Then the obtained PF-*b*-P(HEMA-TMS) (70 mg) was dissolved in 15mL dry THF, KF (5 mg) and TBAF (5 μL) were added to the polymer solution and stirred for 24 h at room temperature. The polymer solution was concentrated under reduced pressure and poured into water. The target copolymer PF-*b*-PHEMA was separated by filtration, and dried under vacuum for 24 h.

Measurements

^{1}H NMR spectra were measured on a BrukerAvance 400 instrument with deuterated chloroform and dimethyl sulfoxide-d_6 as the solvent.

Fourier-transform infrared (FTIR) spectra were obtained on an Avatar 360 FTIR spectrophotometer by dispersing samples in KBr disks.

The molecular weight (Mn) and molecular weight distribution (Mw/Mn, PDI) of the polymers were determined at 40 °C by GPC equipped with a waters 1515 isocratic HPLC pump, three styragel columns (Waters HT4, HT5E, and HT6) and a waters 2414 refractive index detector (set at 30 °C), using THF as the eluent at the flow rate of 1.0 mL/min. A series of polymethyl methacrylate narrow standards were used to generate a conventional calibration curve.

Thermogravimetric analysis (TGA) was conducted on a SDT Q600 under a heating rate of 10 °C/min from room temperature to 800 °C in nitrogen gas atomsphere.

The fluorescence measurement was carried out on a Hitachi 7000 spectrofluorometer with a xenon lamp as a light source.

Water contact angle (WCA) measurements were carried out on a Contact Angle Measuring Instrument (KRUSS, DSA30). The wetting liquid used was water. For each angle reported, at least five sample readings from different surface locations were averaged.

The films used for fluorescence and WCA measurements were prepared as follows. Glass slides were first cleaned successive using acetone, ethyl alcohol and deionized water. The polymer solution (10 mg/ml in THF) was then spin-casted onto clean glass slide at 2000 rpm for 30 s, and dried naturally for 24 h.

Results and discussion

Characterization of polymers structure

According to the relevant literature[29] and our previous work[34], PF-OH (Mn=

5947 g/mol, Mw/Mn = 1.56) was first prepared through a modified Suzuki coupling reaction with 2-bromo-9,9-di-n-hexylfluoreneboronic acid and a 4-bromobenzyl alcohol end-capper. After esterification of PF-OH with 2-bromoisobutyryl bromide, bromo-ended polyfluorene PF-Br was obtained. Mn=6067 g/mol, Mw/Mn = 1.48. The successful synthesis of PF-OH and PF-Br can be confirmed by ^{1}H NMR and FTIR (**Figure S1** and **Figure S2** of the Electronic Supplementary Information).

All polyfluorene-based rod-coil block copolymers were synthesized *via* ATRP method with the bromo-ended polyfluorene as macroinitiator (shown in **Scheme 1**). And their chemical structures were confirmed by ^{1}H NMR and FTIR. **Fig. 1A-a** and **Fig. 1A-b** show the ^{1}H NMR spectra of PF-*b*-PHFBMA and PF-*b*-PBMA respectively. The appearance of peak at 4.42 ppm in **Fig. 1A-a** and peak at 3.95 ppm in **Fig. 1A-b**, corresponding to the protons of the -O-CH_2-CF_2- group of HFBMA and the -O-CH_2- group of BMA, respectively, indicate the successful synthesis of PF-*b*-PHFBMA and PF-*b*-PBMA. The FTIR spectra of PF-*b*-PHFBMA (**Fig. 2 A-a**) and PF-*b*-PBMA (**Fig. 2 A-b**) both exhibit more stronger absorption peak at 1730 cm^{-1} which is assigned to the stretching vibrations of C=O group of PHFBMA and PBMA. These results also confirm the successful synthesis of PF-*b*-PHFBMA and PF-*b*-PBMA (the original ^{1}H NMR and FTIR spectra of PF-Br for comparison are respectively shown in **Figure S1-b** and **Figure S2-b** of the Electronic Supplementary Information).

Fig. 1 B-a and Fig. 2 B-a respectively show the ^{1}H NMR and FTIR spectra of PF-*b*-P*t*BA. The appearance of peak at 1.44 ppm corresponding to the protons of

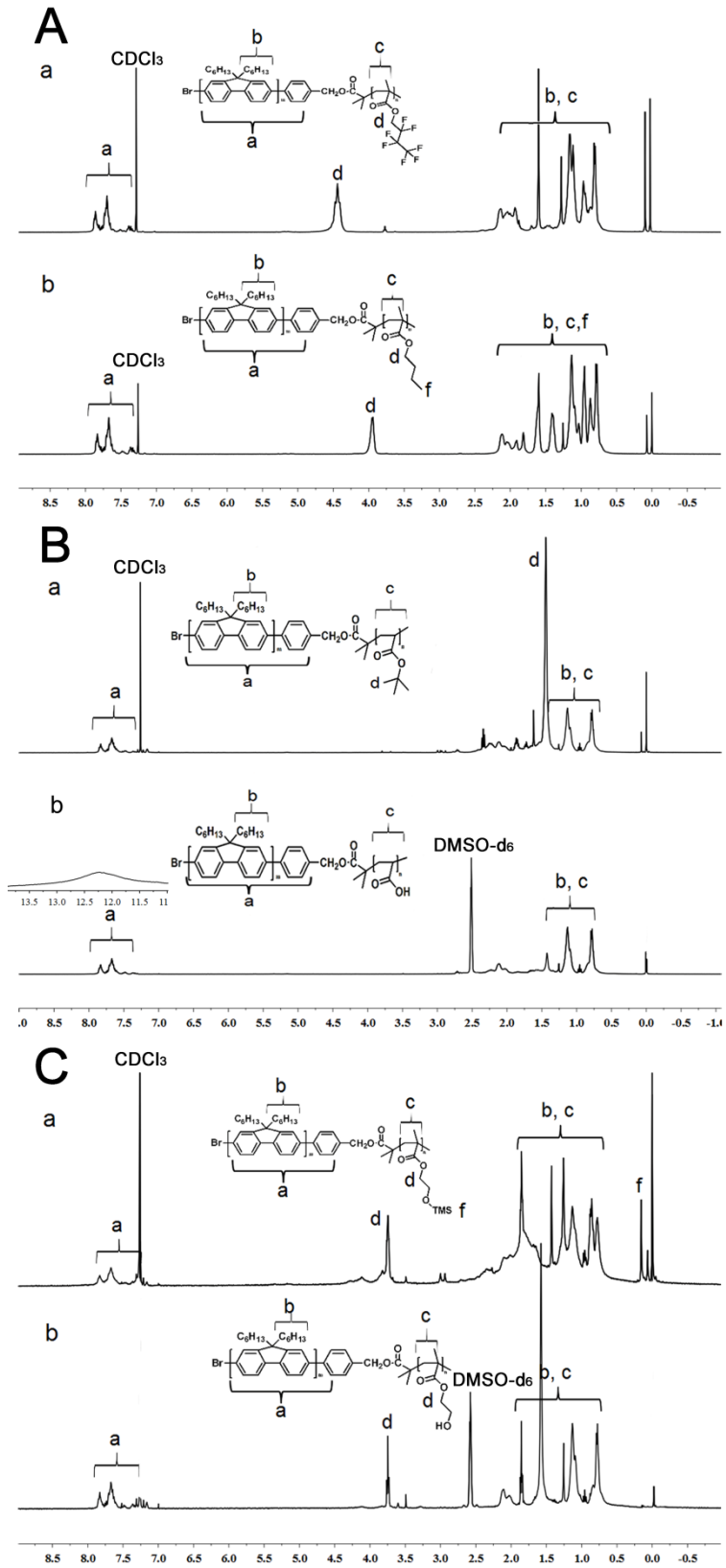

Figure 1. ^{1}H NMR spectra of polyfluorene-based rod-coil block copolymers (A-a) PF-*b*-PHFBMA and (A-b) PF-*b*-PBMA in $CDCl_3$; (B-a) PF-*b*-P*t*BA in $CDCl_3$ and (B-b) PF-*b*-PAA in DMSO-d_6; (C-a) PF-*b*-P(HEMA-TMS) in $CDCl_3$ and (C-b) PF-*b*-PHEMA in DMSO-d_6.

tert-butyl group (**Fig. 1 B-a)** and the more stronger absorption peak at 1730 cm^{-1} which

is assigned to the stretching vibrations of C=O group of P*t*BA (**Fig. 2 B-a**) both indicate the successful synthesis of PF-*b*-P*t*BA. After hydrolysis, the ^{1}H NMR spectrum of PF-*b*-PAA in DMSO (**Fig. 1 B-b**) show the obviously decreases of the tert-butyl resonance at 1.44 ppm and the appearance of the peak at 12.25 ppm assigned to the protons of carboxyl groups. In the FTIR spectrum of PF-*b*-PAA (**Fig. 2 B-b**), a new adsorption peak characteristic of carboxylic acid group appears at 3436 cm^{-1} and the signal at 1370 cm^{-1} attributed to the symmetric bending vibration of the tert-butyl group disappears. These results reveal the successful preparation of PF-*b*-PAA (the original ^{1}H NMR and FTIR spectra of PF-Br for comparison are respectively shown in **Figure S1-b** and **Figure S2-b** of the Electronic Supplementary Information).

The ^{1}H NMR spectra of PF-*b*-PHEMA-TMS and PF-*b*-PHEMA are shown in **Fig. 1C**. In **Fig. 1 C-a**, the appearance of peak at 3.75 ppm corresponding to the protons of the $-CH_2-$ group of $-CH_2-O-Si(CH_3)_3$, and the appearance of peak at 0.16 ppm corresponding to the protons of $-CH_3$ group of $-Si(CH_3)_3$, both indicate the successful incorporation of HEMA-TMS to PF segment. After the deprotection reaction using KF/TBAF as the catalyst, the disappearance of peak at 0.16 ppm (**Fig. 1 C-b**) indicate that the -TMS groups on PHEMA are successful removed. The successful synthesis of PF-*b*-PHEMA also can be confirmed by the appearance of the adsorption peak at 3436 cm^{-1} in **Fig. 2 C-b**, which is assigned to the stretching vibrations of the -OH group of PHEMA (the original ^{1}H NMR and FTIR spectra of PF-Br for comparison are respectively shown in **Figure S1-b** and **Figure S2-b** of the Electronic Supplementary Information).

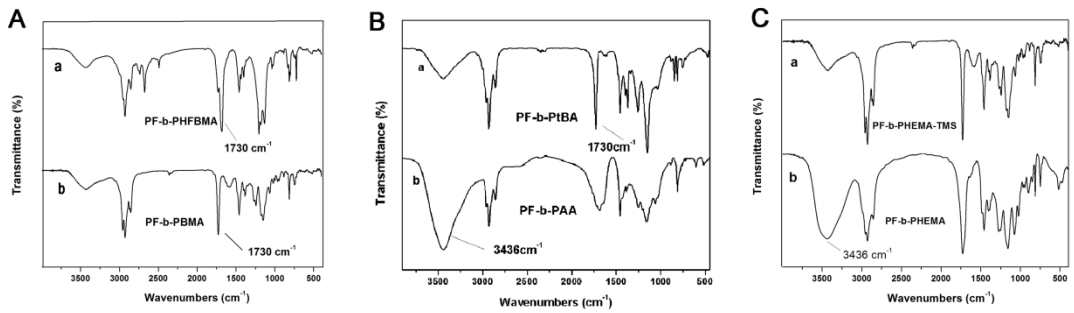

Figure 2. FTIR spectra of polyfluorene-based rod-coil block copolymers (A-a) PF-*b*-PHFBMA and (A-b) PF-*b*-PBMA; (B-a) PF-*b*-P*t*BA and (B-b) PF-*b*-PAA; (C-a) PF-*b*-P(HEMA-TMS) and (C-b) PF-*b*-PHEMA.

Fig. 3 shows the GPC traces for the four as-prepared copolymers. The relatively narrow polydispersity indicates the good controllability of polymerization. However, the results of PF-*b*-PHFBMA seem to be unusual, which might be due to the collapsed coil structure of PHFBMA block in THF.[34] Additionally, the molecular weights of PF-*b*-PHEMA (Mn=13137 g/mol) and PF-*b*-PAA (Mn=10502 g/mol) can be calculated by the results of PF-*b*-PHEMA-TMS and PF-*b*-P*t*BA, since PF-*b*-PHEMA-TMS and PF-*b*-P*t*BA exhibit better solubility in THF eluent.

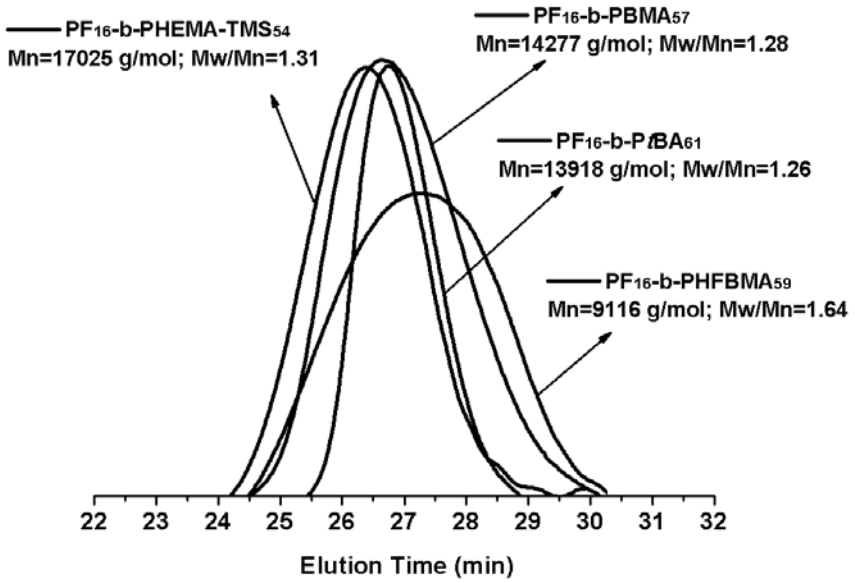

Figure 3. GPC traces of polyfluorene-based rod-coil block copolymers PF-*b*-PHFBMA, PF-*b*-PBMA, PF-*b*-P(HEMA-TMS), PF-*b*-P*t*BA.

The influence of annealing on the spectral stability of polymers

It is well known that the formation of fluorenone defect structure might affect the spectral stability of polymers during the polymerization of fluorene monomer. Therefore, the hydroxyl-ended polyfluorene was prepared in the dark. The ^{13}C NMR spectrum of PF-OH in **Fig. 4** shows that the characteristic peak at δ=194 ppm corresponding to carbonyl is absence, which confirms that fluorenone defects are prevented successfully during the reaction.[36]

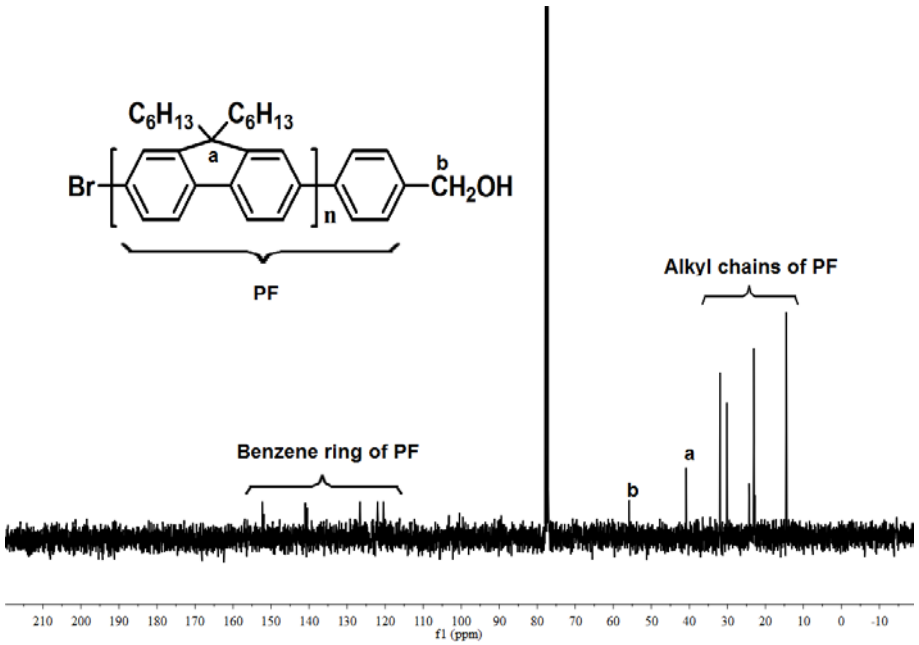

Figure 4. ^{13}C NMR Spectra of PF-OH in $CDCl_3$.

After excluding the impact of fluorenone defects, the effect of incorporating different coil segments on the spectral stability of polyfluorene-based copolymers have been investigated under different thermal treatment conditions, including annealing temperature, annealing time and annealing atmosphere. Green index φ, defined as intensity ratio of green emission (~530nm) to the strongest peak of the blue emission (I_{green}/I_{blue}),[37,38] was introduced to depict the low-energy emission. The larger the value of φ is, the stronger the low-energy emission is, which indicates the poorer

the spectral stability.

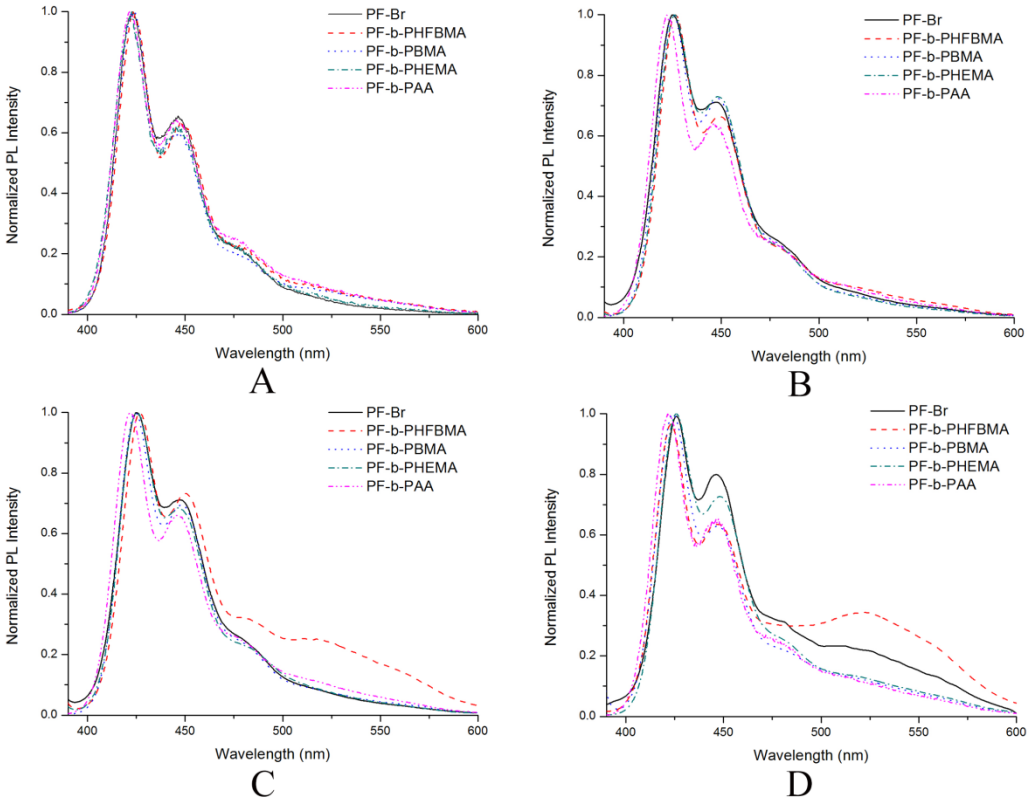

Figure 5. Fluorescence spectra of PF-Br, PF-*b*-PHFBMA, PF-*b*-PBMA, PF-*b*-PHEMA and PF-*b*-PAA films (A) annealed 1h at 50 °C in air, (B) annealed 1h at 100 °C in air, (C) annealed 1h at 150 °C in air and (D) annealed 1h at 200 °C in air.

First, the spectral stability of polyfluorene-based polymers under different annealing temperature for 1h was investigated. From the results shown in **Fig. 5 (A)-(D)**, no new emission band appears in the spectra of PF-Br, PF-*b*-PHFBMA, PF-*b*-PBMA, PF-*b*-PHEMA and PF-*b*-PA when the annealing temperature is 50 °C or 100 °C. As the temperature increases to 150 °C, emission band at 525nm only appears in the spectrum of PF-*b*-PHFBMA, the green index φ=0.25. When the temperature continues increasing to 200 °C， this emission band is also observed in the case of PF-Br, the green index φ=0.23, simultaneously, the intensity of this emission band in the spectrum of PF-*b*-PHFBMA increases significantly, the green index φ=0.34 . As a whole, the annealing temperature has influence on the spectral stability to some

extent.

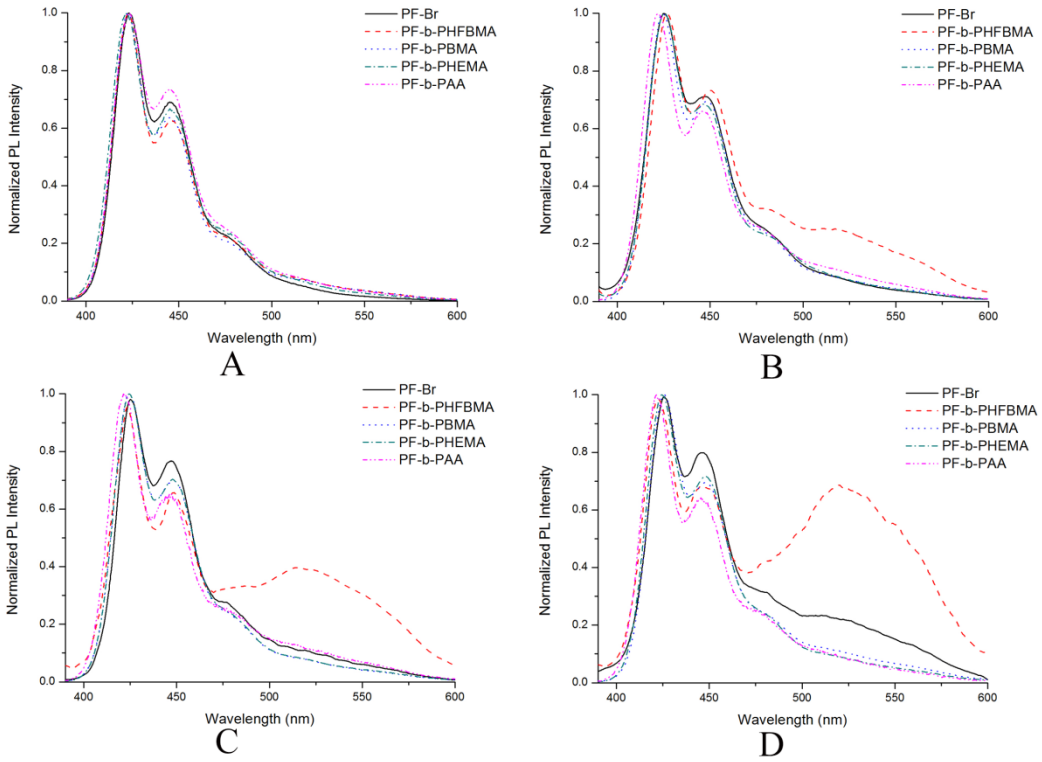

Figure 6. Fluorescence spectra of PF-Br, PF-*b*-PHFBMA, PF-*b*-PBMA, PF-*b*-PHEMA and PF-*b*-PAA fims (A) pristine spin-cast, (B) annealed 1h, (C) annealed 3h and (D) annealed 6h at 150 °C in air.

Fig. 6 (**A**)-(**D**) show the spectra of polyfluorene-based polymers PF-Br, PF-*b*-PHFBMA, PF-*b*-PBMA, PF-*b*-PHEMA and PF-*b*-PAA under different annealing time at 150 °C in air. When the annealing time is 1h, the emission band at 525 nm only appears in the spectrum of PF-*b*-PHFBMA, the green index φ=0.25 (**Fig. 6** (**B**)). As the annealing time go on，the spectra of PF-*b*-PBMA, PF-*b*-PHEMA and PF-*b*-PAA still maintain steady while the emission band at 525 nm is observed in the spectrum of PF-Br at 6h, the green index φ=0.22 (**Fig. 6** (**D**)). The intensity of the emission band at 525 nm appeared in the spectrum of PF-*b*-PHFBMA increases significantly (φ=0.69) as the annealing time increase to 6h (**Fig. 6** (**D**)). The above results suggest that polyfluorene can maintain the spectral stability in a short period

annealing time. However, when the annealing time exceeds a certain value, low-energy emission begin to appear. In a word, introducing the coil blocks PBMA, PHEMA and PAA can improve the spectral stability of polyfluorene while incorporating the coil block PHFBMA has the opposite effect.

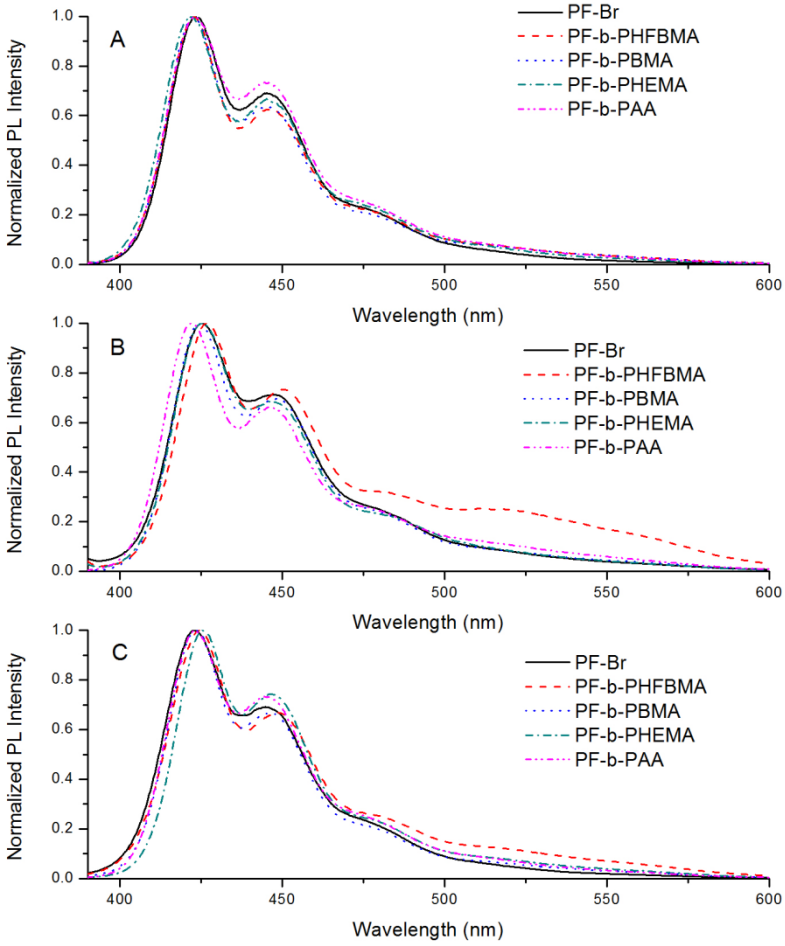

Figure 7. Fluorescence spectra of PF-Br, PF-*b*-PHFBMA, PF-*b*-PBMA, PF-*b*-PHEMA and PF-*b*-PAA films (A) pristine spin-cast, (B) annealed 1h at 150 °C in air, (C) films annealed 1h at 150 °C in vacuum.

To confirm whether the fluorenone defect structure was formed due to annealing in air, the spectral stability of polyfluorene-based polymers in different atmosphere at

150 °C for 1h was investigated. The corresponding emission spectra are depicted in **Fig. 7**. By compared to the pristine spin-casted film, no low-energy emission is present in the spectra of PF-Br, PF-*b*-PBMA, PF-*b*-PHEMA and PF-*b*-PAA either in vacuum or in air. In contrast, PF-*b*-PHFBMA exhibits the 525nm emission band in air and in vacuum. From the results above, we suppose that the fluorenone defect structure might not form in air due to the limited oxidation in solid state, and the low-energy emission of PF-*b*-PHFBMA film might be resulted from molecular aggregation.

In combination with the results discussed above, both PF-Br and PF-*b*-PHFBMA exhibit the 525nm low-energy emission band after annealing in air at 200 °C for 1h (**Fig. 5** (**D**)) or at 150 °C for 6h (**Fig. 6** (**D**)). The ^{13}C NMR spectrum of PF-OH (**Fig. 4**) and the spectra of rod-coil copolymer films annealed in vacuum (**Fig. 7** (**C**)) excluding the impact of fluorenone defects on the spectral stability of polyfluorene-based polymer. Therefore, we tentatively suggest that introducing the coil blocks PBMA, PHEMA and PAA can inhibit the low-energy emission of polyfluorene while incorporating the coil block PHFBMA has the opposite effect, and aggregation behavior between fluorene chain is the cause of the low-energy emission band.

To PF-*b*-PHFBMA, the unfavorable enthalpic interactions between the fluorinated segment and the PF block can drive the segregation of copolymer. During the segregation process, PHFBMA is oriented to gather on the air-polymer surface due to its low surface free energy and self-aggregated property. If the annealing

temperature is constant, the amount of fluorinated segments on the surface will increase gradually with the increase of annealing time, and finally reached a maximal value.[39,40] The accompanied aggregation of PF blocks on the other side causes the low-energy emission band, and the intensity of the emission gradually increase as the annealing time go on (**Fig. 6**). The increase of the annealing temperature can promote the moving of PHFBMA segments and the aforementioned maximal surface value can be reached in a shorter period time when the temperature is higher.[39,40] It is a reasonable explanation about the appearance of low-energy emission band and the enhanced intensity of the emission as the increase of the annealing temperature (**Fig. 5**). Compared with PHFBMA block, PBMA, PHEMA and PAA blocks have a better compatibility with PF, the separation trend of copolymers PF-*b*-PBMA, PF-*b*-PHEMA and PF-*b*-PAA are relatively weaker. Aggregation of PF blocks is less likely to occur even at a relative high temperature. Therefore, increasing annealing temperature or extending annealing time, a low-energy emission band never appear in the spectra of the polyfluorene-based copolymers with PBMA, PHEMA and PAA as coil blocks (**Figs. 5 and 6**).

Surface properties

The further investigation about the surface properties of as-prepared films is to gain some supporting information for the above conclusion. By comparison of the results obtained before and after annealing at 150 °C in air for 1h, one can find that the WCA of PF-*b*-PHFBMA film increases from 107° to 113° and the other as-prepared films have no distinct difference in **Fig. 8 A** and **B**. The phenomenon

confirmed the fact that fluorinated blocks are prefer to migrate onto the surface of film, and the accompanied aggregation of PF blocks on the other side will causes the low-energy emission band. These provide the supporting information for the spectral instability of PF-*b*-PHFBMA film.

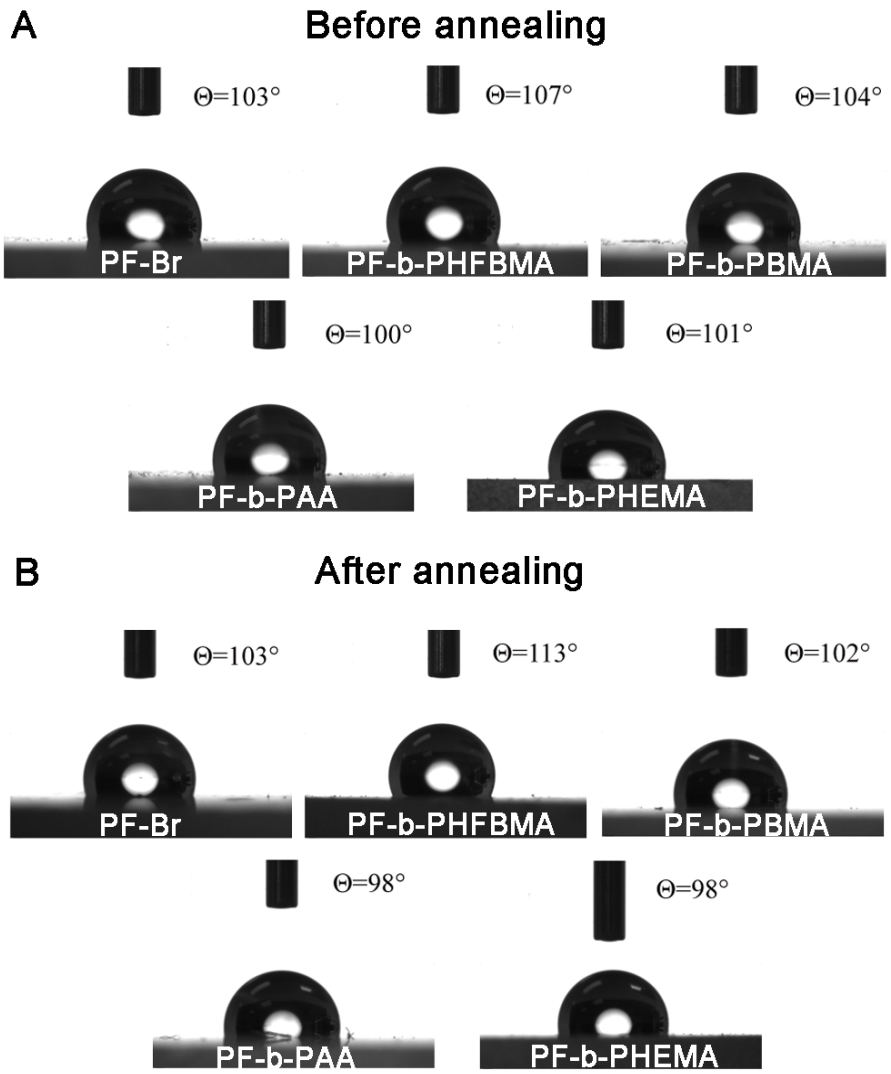

Figure 8. The static WCA images of films (A) before annealing and (B) after annealing at 150 °C in air for 1h.

Thermal properties

The thermal behavior of the initiator PF-Br and the polyfluorene-based rod-coil block copolymers were studied using TGA (**Fig. 9**). It is evident from **Fig. 9** that

PF-Br presents two thermal degradation temperatures at 225 °C and 425 °C, which

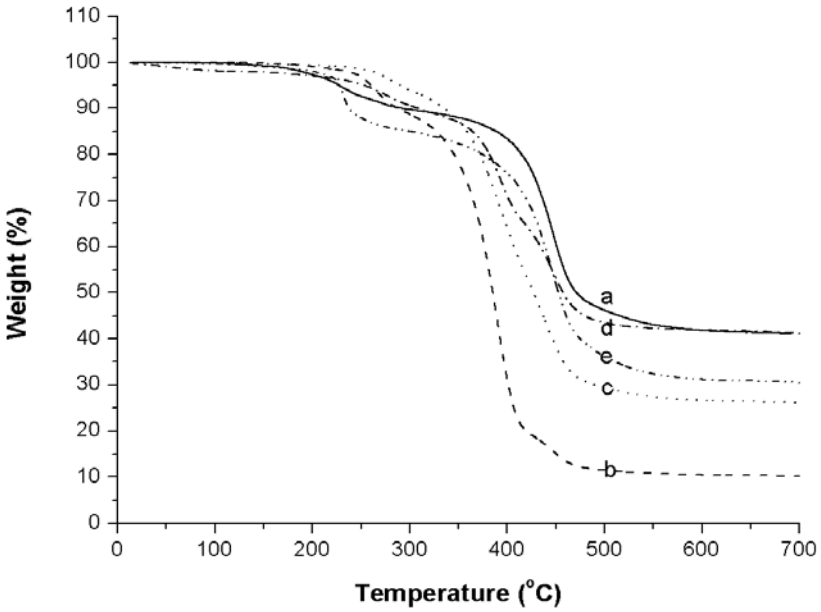

Figure 9. TGA curves of (a) PF-Br, (b) PF-*b*-PHFBMA, (c) PF-*b*-PBMA, (d) PF-*b*-PHEMA and (e) PF-*b*-PAA.

are attributed to the decomposition of the micromolecules and polyfluorene, respectively. The rest weight percentage of PF at 700 °C is 41.4%. Block copolymers PF-*b*-PHFBMA, PF-*b*-PBMA, PF-*b*-PHEMA and PF-*b*-PAA undergo two-step decompositions, the flexible-coil blocks first decomposition under a lower temperature (225℃-330℃). Subsequently, the PF rod segments begin to decompose from 350 ℃ to 500℃. Their rest weight percentage at 700 °C are 10.2%, 26.1%, 41.1% and 30.5%, respectively. The thermal degradation temperatures of polyfluorene-based rod-coil block copolymers decrease slightly compared to PF-Br, indicating that the incorporation of coil blocks with polyfluorene have a negative effect on the thermal stability of the polymers. However, these rod-coil block copolymers still are thought to be good thermal stability within the slightly reduction.

Conclusion

A series of polyfluorene-based rod-coil block copolymers, including PF-*b*-PHFBMA, PF-*b*-PBMA, PF-*b*-PHEMA and PF-*b*-PAA, were synthesized *via* ATRP technique using PF-Br as macroinitiator. The macroinitiator was prepared through modified Suzuki coupling reaction and esterification. The structures of resulted copolymers were confirmed by the ^{1}H NMR and FTIR spectra. The investigations about spectral stability of polyfluorene-based rod-coil block copolymers under different thermal treatment operations demonstrate that incorporating the coil blocks PBMA, PHEMA and PAA can prevent the low-energy band emission while the coil block PHFBMA produce the opposite effect on the spectral stability. A proper coil block is essential for the stabilization of the emission spectra of polyfluorene-based copolymers. Simultaneously, after excluding the impact of fluorenone defects, aggregation behavior between fluorene chains is considered to the cause of the low-energy emission band. Furthermore, surface properties of copolymers are used to further explore the supporting information for the spectral instability of PF-*b*-PHFBMA film.

The thermal behaviors of all polymers investigated by TGA indicate that incorporation of coil blocks with polyfluorene does not much affect the thermal properties of polymers, which can be used to prepare the electronic device with inhibited low-energy emission.

Acknowledgments

The authors thank the National Ministry of Science and Technology of China (No.

2012CB21500402) and the National Natural Science Foundation of China (No. 21076171, 21276213) for supporting this work.

Notes and References

1 G. Z. Yang, P. Chen, T. X. Liu, M. Wang and W. Huang, *Polym. Adv. Technol.*, 2006, **17**, 544-551.

2 G. Z. Yang, M. Wu, S. Lu, M. Wang, T. X. Liu and W. Huang, *Polymer*, 2006, **47**, 4816-4823.

3 G. Z. Yang, W. Z.Wang, M. Wang and T. X. Liu, *J. Phys. Chem. B*, 2007, **111**, 7747-7755.

4 A. Farcas, S. Janietz, V. Harabagiu, P. Guegan and P. H. Aubert, *J. Polym. Sci. Polym. Chem.*, 2013, **51**, 1672-1683.

5 G. Zeng, W. L. Yu, S. J. Chua and W. Huang, *Macromolecules*, 2002, **35**, 6907-6914.

6 U. Scherf and E. J. W. List, *Adv. Mater.*, 2002, **14**, 477-487.

7 M. Gaal, E. J. W. List and U.Scherf, *Macromolecules*, 2003, **36**, 4236-4237.

8 L. Romanner, A. Pogantsch, P. Scandiucci de Freitas, U. Scherf, M. Gaal, E. Zojer and E. J. W. List, *Adv. Funct. Mater*., 2003, **13**, 597-601.

9 A. De Cuendias, M. Le Hellaye, S. Lecommandoux, E. Cloutet and H. Cramail, *J. Mater. Chem.*, 2005, **15**, 3264-3267.

10 W. Y. Wong, L. Liu, D. M. Cui, L. M. Leung, C. F. Kwong, T. H. Lee and H. F. Ng, *Macromolecules*, 2005, **38**, 4970-4976.

11 A. P. Kulkarni, Y. Zhu and S. A. Jenekhe, *Macromolecules*, 2005, **38**, 1553-1563.

12 Y. S. Wu, J. Li, X. C. Ai, L. M. Fu, J. P. Zhang, Y. Q. Fu, J. J. Zhou, L. Li and Z. S. Bo, *J. Phys. Chem. A*, 2007, **111**, 11473-11479.

13 X. H. Zhou, Y. Zhang, Y. Q. Xie, Y. Cao and J. Pei, *Macromolecules*, 2006, **39**,

3830-3840.

14 C. L. Chochos and S. A. Choulis, *Prog. Polym. Sci.*, 2011, **36**, 1326-1414.

15 K. Asai, G. Konishi, K. Sumi and S. Kawauchi, *Polym. Chem.*, 2010, **1**, 321-325

16 H. Yeo, K. Tanaka and Y. Chujo, *J. Polym. Sci. Polym. Chem.*, 2012, **50**, 4433-4442.

17 G. E. McCluskey, S. E. Watkins, A. B. Holmes, C. K. Ober, J. K. Lee and W. W. H. Wong, *Polym. Chem.*, 2013, **4**, 5291–5296.

18 S. Beaupre, M. Ranger and M. Leclerc, *Macromol. Rapid Commun.*, 2000, **21**, 1013-1016.

19 M. R. Craig, M. M. de Kok, J. W. Hofstraat, A. P. H. J. Schenning and E. W. Meijer, *J. Mater. Chem.*, 2003, **13**, 2861-2868.

20 P. Kulkarni and S. A.Jenekhe, *Macromolecules*, 2003, **36**, 5285-5291.

21 L. H. Xie, C. R. Yin, W. Y. Lai, Q. L. Fan and W. Huang, *Prog. Polym. Sci.*, 2012, **37**, 1192-1264.

22 Y. Q. Tian, C. Y. Chen, H. L. Yip, W. C. Wu, W. C. Chen and A. K. Y. Jen, *Macromolecules*, 2010, **43**, 282-291.

23 S. Lu, T. X. Liu, L. Ke, D. G. Ma, S. J. Chua and W. Huang, *Macromolecules*, 2005, **38**, 8494-8502.

24 C. L. Chochos, J. K. Kallitsis, P. E. Keivanidis, S. Baluschev and V. G. Gregoriou, *J. Phys. Chem. B*, 2006, **110**, 4657-4662.

25 C. L. Chochos, N. P. Tzanetos, S. P. Economopoulos, V. G. Gregoriou and J. K. Kallitsis, *Eur. Polym. J.*, 2007, **43**, 5065-5075.

26 Y. K. Kwon, H. S. Kim, H. J. Kim, J. H. Oh, H. S. Park, Y. S. Ko, K. B. Kim and M. S. Kim, *Macromolecules*, 2009, **42**, 887-891.

27 Y. C. Tung, W. C. Wu and W. C. Chen, *Macromol. Rapid Commun.*, 2006, **27**,

1838-1844.

28 S. T. Lin, Y. C. Tung and W. C. Chen, *J. Mater. Chem.*, 2008, **18**, 3985-3992.

29 Y. C. Tung and W. C. Chen, *React. Funct. Polym.*, 2009, **69**, 507-518.

30 C. C. Kuo, Y. C. Tung, C. H. Lin and W. C. Chen, *Macromol. Rapid Commun.*, 2008, **29**, 1711-1715.

31 C. L. Liu, C. H. Lin, C. C. Kuo, S. T. Liu and W. C. Chen, *Prog. Polym. Sci.*, 2011, **36**, 603-637.

32 X. D. Lou, Y. Zhang, S. Li, D. X. Ou, Z. M. Wan, J. G. Qin and Z. Li, *Polym. Chem.*, 2012, **3**, 1446-1452.

33 C. S. Wu, C. T. Liu and Y. Chen, *Polym. Chem.*, 2012, **3**, 3308-3317.

34 J. J. Wang, Y. N. Zhou, P. Wang and Z. H. Luo, *Rsc Adv.*, 2013, **3**, 5045-5055.

35 K. L. Beers, S. Boo, S. G. Gaynor and K. Matyjaszewski, *Macromolecules*, 1999, **32**, 5772-5776.

36 X. Gong, P. K. Iyer, D. Moses, G. C. Bazan, A. J. Heeger and S. S. Xiao, *Adv. Funct. Mater.*, 2003, **13**, 325–330.

37 W. Zhao, T. Cao and J. M. White, *Adv. Funct. Mater.*, 2004, **14**, 783-790.

38 X. Y. Hou, T. C. Li, J. Liang, D. Y. Chen, L. H. Xie and W. Huang, *Acta Chim Sin*, 2008, **66**, 2575-2578.

39 K. Li, P. Wu and Z. Han, *Polymer*, 2002, **43**, 4079-4086.

40 I. J. Park, S. B. Lee, C. K. Choi and K. J. Kim, *J. Colloid Interface Sci.*, 1996, **181**, 284-288.

Graphic Abstract

Spectral stability of polyfluorene-based copolymers could be improved through incorporating an appropriate coil segment.

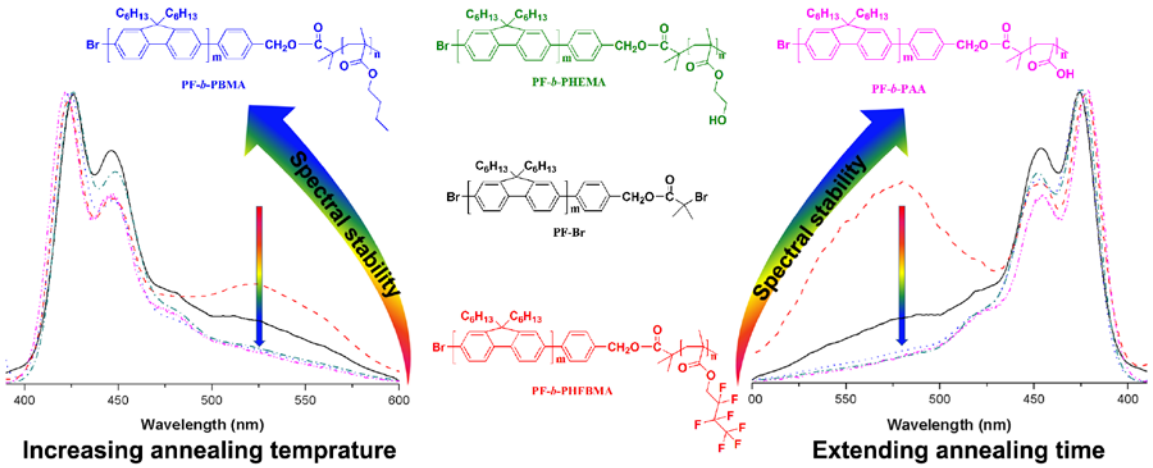

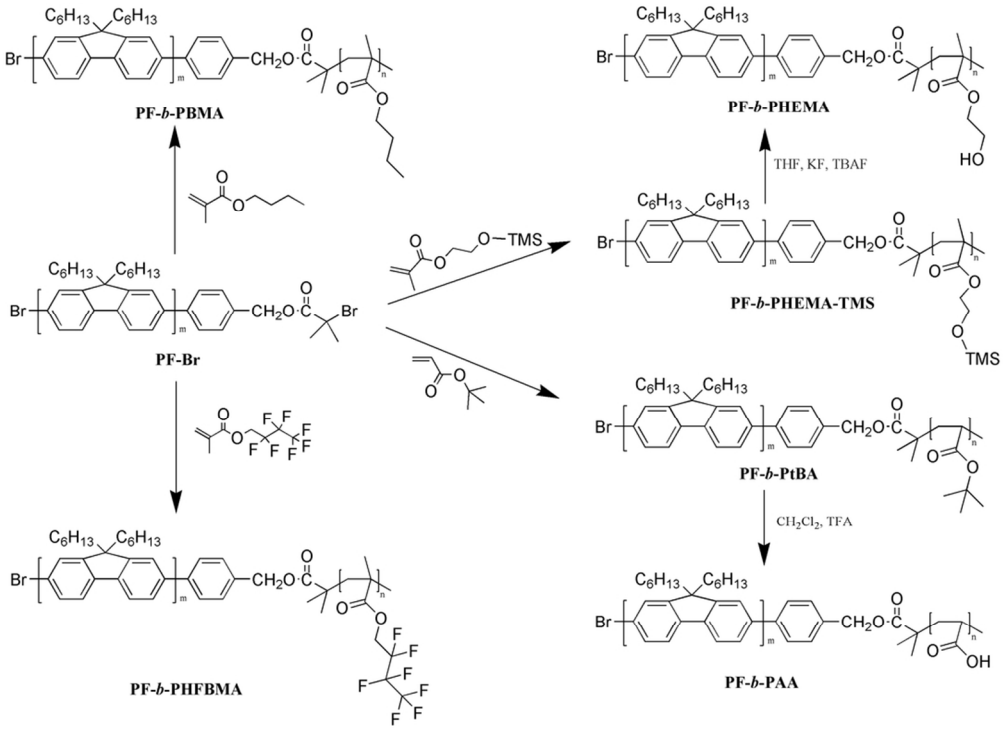

Scheme 1. Synthesis Route of polyfluorene-based rod-coil block copolymers PF-b-PHFBMA, PF-b-PBMA, PF-b-PHEMA, PF-b-PAA.
45x33mm (600 x 600 DPI)

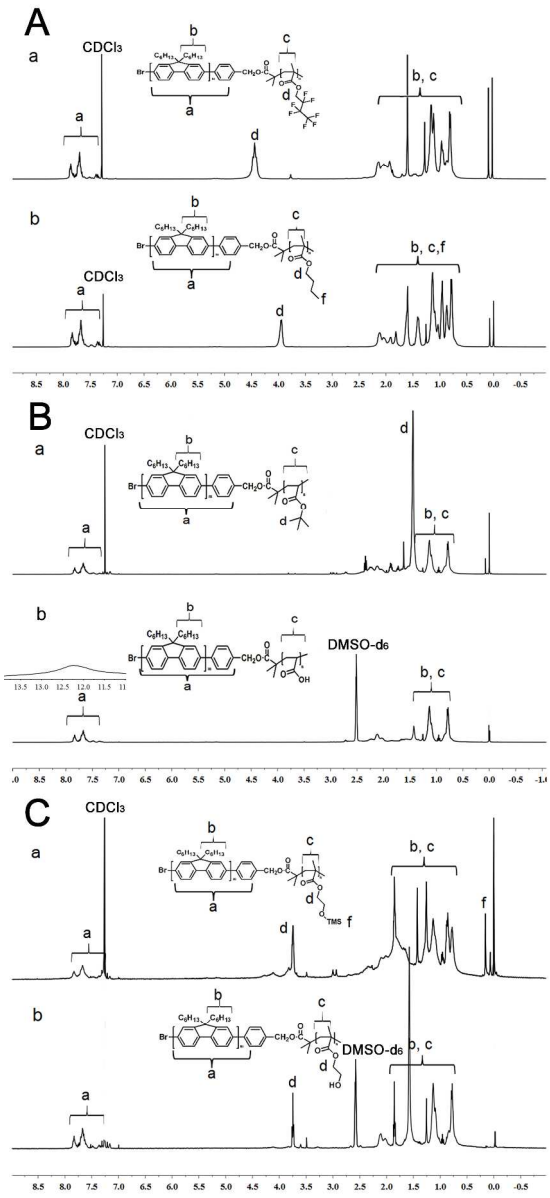

Figure 1. 1H NMR spectra of polyfluorene-based rod-coil block copolymers (A-a) PF-b-PHFBMA and (A-b) PF-b-PBMA in CDCl3; (B-a) PF-b-PtBA in CDCl3 and (B-b) PF-b-PAA in DMSO-d6; (C-a) PF-b-P(HEMA-TMS) in CDCl3 and (C-b) PF-b-PHEMA in DMSO-d6.
138x300mm (600 x 600 DPI)

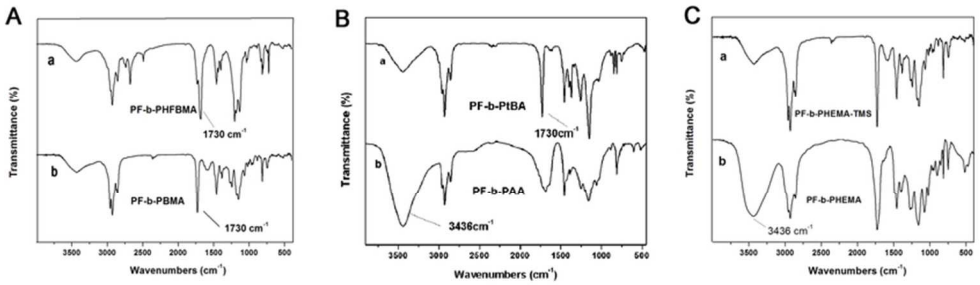

Figure 2. FTIR spectra of polyfluorene-based rod-coil block copolymers (A-a) PF-b-PHFBMA and (A-b) PF-b-PBMA; (B-a) PF-b-PtBA and (B-b) PF-b-PAA; (C-a) PF-b-P(HEMA-TMS) and (C-b) PF-b-PHEMA
36x10mm (600 x 600 DPI)

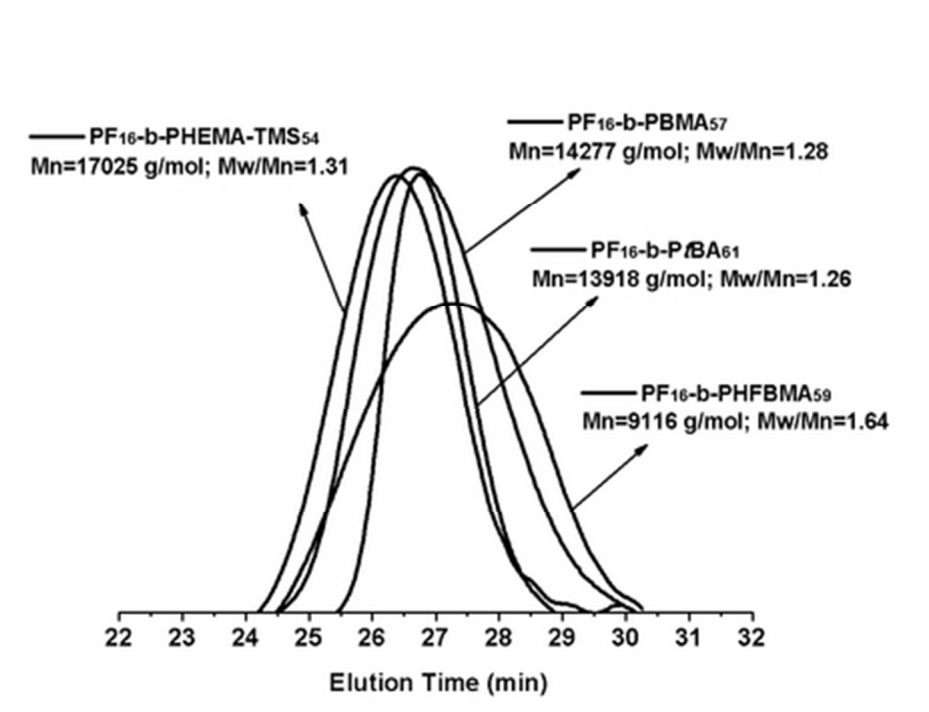

Figure 3. GPC traces of polyfluorene-based rod-coil block copolymers PF-b-PHFBMA, PF-b-PBMA, PF-b-P(HEMA-TMS), PF-b-PtBA.
19x15mm (600 x 600 DPI)

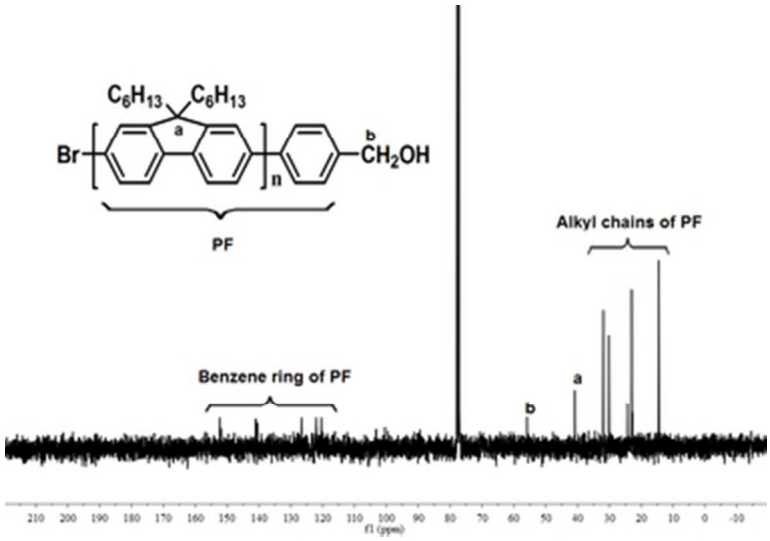

Figure 4. 13C NMR Spectra of PF-OH in CDCl3.
16x11mm (600 x 600 DPI)

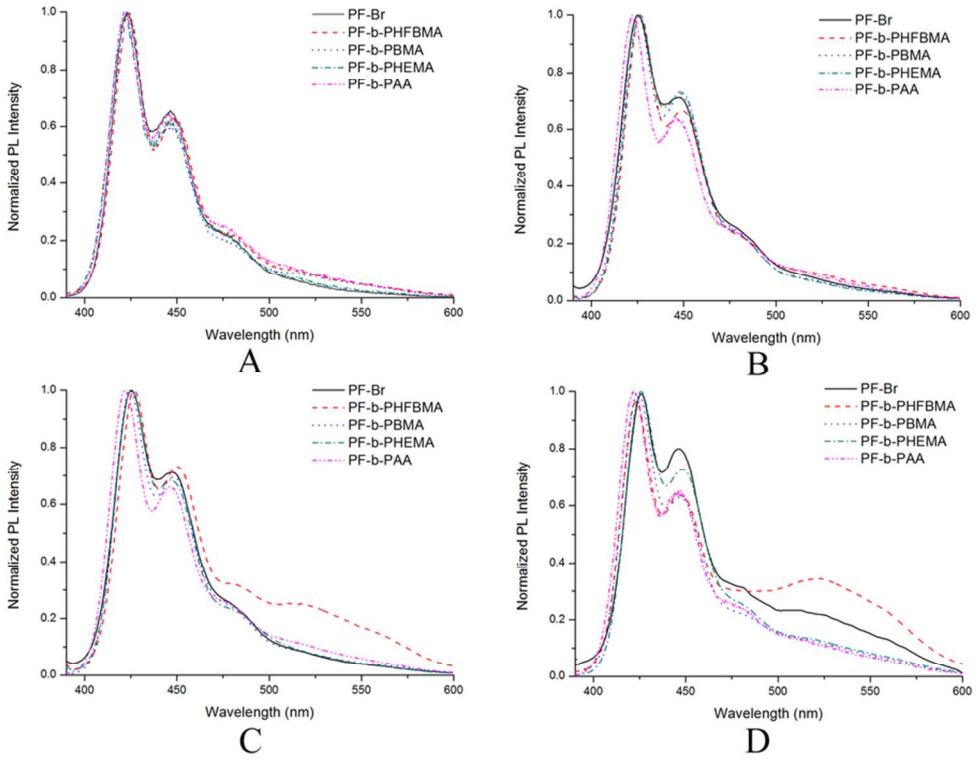

Figure 5. Fluorescence spectra of PF-Br, PF-b-PHFBMA, PF-b-PBMA, PF-b-PHEMA and PF-b-PAA films (A) annealed 1h at 50℃ in air, (B) annealed 1h at 100℃ in air, (C) annealed 1h at 150℃ in air and (D) annealed 1h at 200℃ in air.
39x30mm (600 x 600 DPI)

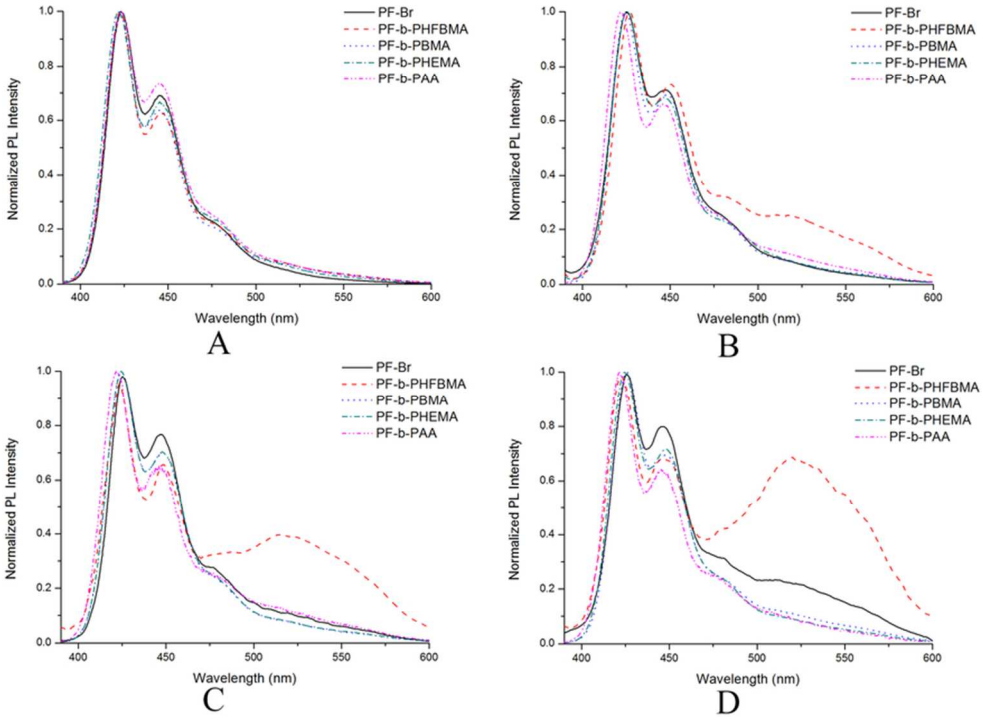

Figure 6. Fluorescence spectra of PF-Br, PF-b-PHFBMA, PF-b-PBMA, PF-b-PHEMA and PF-b-PAA fims (A) pristine spin-cast, (B) annealed 1h, (C) annealed 3h and (D) annealed 6h at 150℃ in air.
37x28mm (600 x 600 DPI)

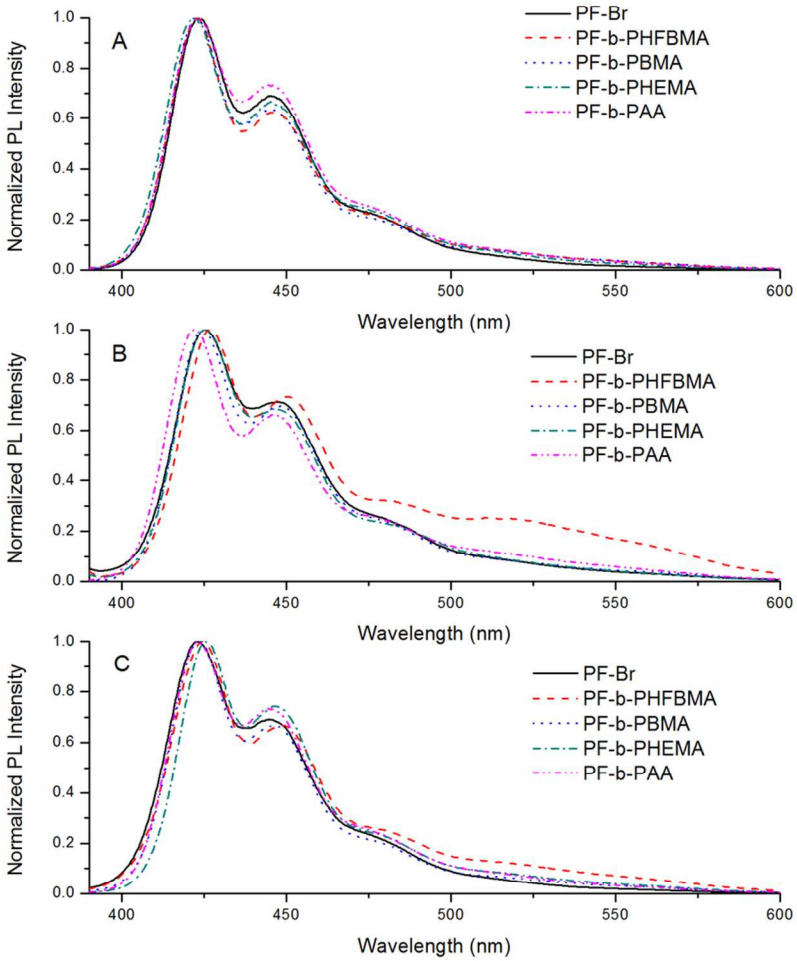

Figure 7. Fluorescence spectra of PF-Br, PF-b-PHFBMA, PF-b-PBMA, PF-b-PHEMA and PF-b-PAA films (A) pristine spin-cast, (B) annealed 1h at 150℃ in air, (C) films annealed 1h at 150℃ in vacuum.
43x56mm (600 x 600 DPI)

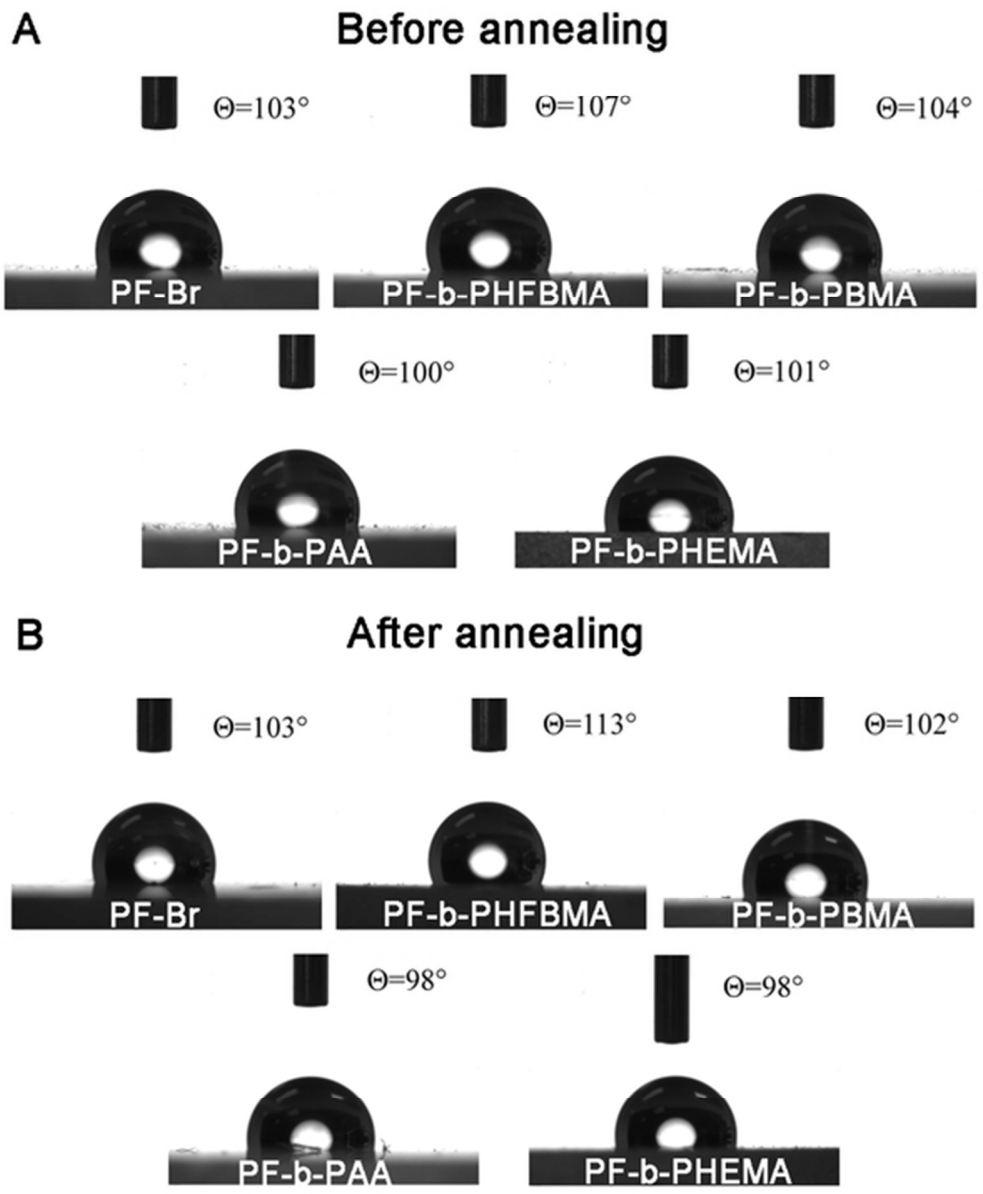

Figure 8. The static WCA images of films (A) before annealing and (B) after annealing at 150℃ in air for 1h.
25x30mm (600 x 600 DPI)

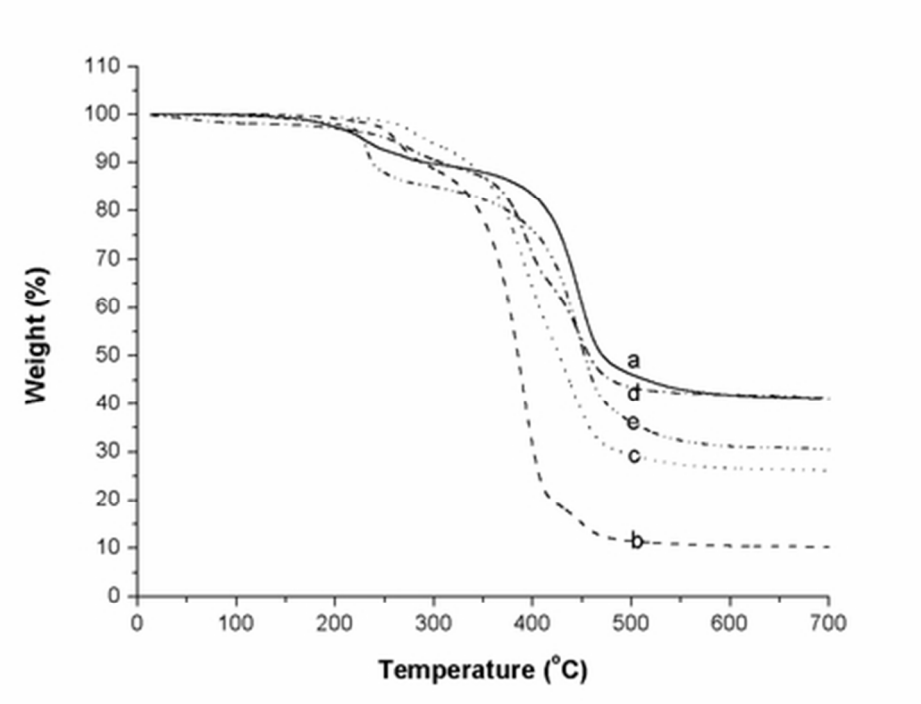

Figure 9. TGA curves of (a) PF-Br, (b) PF-b-PHFBMA, (c) PF-b-PBMA, (d) PF-b-PHEMA and (e) PF-b-PAA.
19x14mm (600 x 600 DPI)

Graphic Abstract

Spectral stability of polyfluorene-based copolymers could be improved through incorporating an appropriate coil segment.